Author Manuscript
Author Manuscript
Author Manuscript
Author Manuscript

HHS Public Access
Author manuscript
Mol Biosyst. Author manuscript; available in PMC 2018 November 21.

Published in final edited form as:
Mol Biosyst. 2017 November 21; 13(12): 2660–2671. doi:10.1039/c7mb00498b.

The nucleosomal surface is the main target of histone ADP-ribosylation in response to DNA damage

Kelly R. Karch[1], **Marie-France Langelier**[2], **John M. Pascal**[2], and **Benjamin A. Garcia**[1]

[1]Department of Biochemistry and Molecular Biophysics, Epigenetics Institute, Perelman School of Medicine, University of Pennsylvania, Philadelphia, PA

[2]Department of Biochemistry and Molecular Medicine, Université de Montréal, Montréal, Qc, Canada

Abstract

ADP-ribosylation is a protein post-translational modification catalyzed by ADP-ribose transferases (ARTs). ART activity is critical in mediating many cellular processes, and is required for DNA damage repair. All five histone proteins are extensively ADP-ribosylated by ARTs upon induction of DNA damage. However, how these modifications aid in repair processes is largely unknown, primarily due to lack of knowledge about where they site-specifically occur on histones. Here, we conduct a comprehensive analysis of histone Asp/Glu ADP-ribosylation sites upon DNA damage induced by dimethyl sulfate (DMS). We also demonstrate that incubation of cell nuclei with NAD+, as has been done previously in the literature, leads to spurious ADP-ribosylation levels of histone proteins. Altogether, we were able to identify 30 modification sites, 20 of which are novel. We also quantify the abundance of these modification sites during the course of DNA damage insult to identify which sites are critical for mediating repair. We found that every quantifiable site increases in abundance over time and that each identified ADP-ribosylation site is located on the surface of the nucleosome. Together, the data suggest specific Asp/Glu residues are unlikely to be critical for DNA damage repair and rather that this process is likely dependent on ADP-ribosylation of the nucleosomal surface in general.

Introduction

ADP-ribosylation is a post-translational modification (PTM) that occurs on a wide variety of proteins throughout the cell. ADP-ribosylation is catalyzed by a class of enzymes called ADP-ribose transferases (ARTs) that use NAD+ as a cofactor to donate an ADP-ribose unit to an acceptor side chain.[1] Lys, Arg, Glu, Asp, and Ser have been previously reported to be acceptors of this PTM.[2–7] ARTs can add single ADP-ribose units to an acceptor protein (mono-ADP-ribosylation, MARylation), or undergo several successive catalytic cycles to generate longer ADP-ribose chains on a single acceptor site (poly-ADP-ribosylation, PARylation). PARylation is a highly heterogeneous modification as it contains varying numbers of ADP-ribose units and can exist as linear chains or highly branched structures.[1]

ADP-ribosylation, especially PARylation, can dramatically alter the function of the acceptor protein, either by directly altering protein chemistry and structure or by altering its network of interacting proteins.[8] In fact, many “reader” domains have been identified that can bind

Author Manuscript Author Manuscript Author Manuscript Author Manuscript

ADP-ribosylated proteins to mediate various cellular processes, including differentiation, transcription, and stress response.[9] One of the most well-studied roles of this modification is in DNA damage repair and maintenance of genome integrity. Some ARTs, such as PARP-1 and PARP-2, can bind directly to single and double strand DNA breaks to initiate repair.[10,11] PARP-1, whose activity increases about 500-fold upon binding to DNA lesions, has been shown to be critical for these repair processes.[12,13]

Histone proteins are one of the most prominent acceptors of ADP-ribosylation in the cell. Histone proteins are responsible for regulating many vital nuclear processes such as transcription, maintenance of higher order chromatin structure, and cellular division. Histones mediate these processes in structures called nucleosomes, which contain 147 base pairs of DNA wrapped around an octamer of histones containing 2 copies of each core histone: H2A, H2B, H3, and H4.[14] A fifth histone, H1, can bind linker DNA between adjacent nucleosomes.[15] As a non-enzymatic protein, histone function is generally mediated by an extensive and dynamic array of post-translational modifications, the most well studied of which include acetylation, methylation, and phosphorylation.[16]

Previous work has revealed that all five histone proteins can be ADP-ribosylated.[2,6,17–20] In order to elucidate how histone ADP-ribosylation is involved in DNA damage response and repair, it is important to first understand where the modifications occur during this process. However, ADP-ribosylation is a particularly challenging PTM to identify for several reasons: (1) it is highly heterogeneous, i.e. variable numbers of ADP-ribose units can be added to a given acceptor site; (2) each ADP-ribose unit imparts 2 negative charges to the molecule; and (3) the PTM is relatively labile. Although ADP-ribosylation was discovered in the 1950s, these challenges precluded comprehensive analysis of histone ADP-ribosylation sites for decades. However, a few sites were identified *in vivo* using mutagenesis and chemical susceptibility approaches.[19,21–23] These sites, which include H1E2 and H1E15, are often considered to be canonical histone ADP-ribosylation sites since they have been known to exist for decades.[21]

In recent years, mass spectrometry (MS) has proven to be a valuable tool to discover and characterize ADP-ribosylation on proteins. However, to implement MS, the ADP-ribosylation sites must first be modified to reduce heterogeneity and impart a single distinct mass shift at each modification site. Some studies have used enzymes to digest the modification to a single small tag. For example, phosphodiesterase (PDE) and Nudix hydrolyases have been used to digest PAR to a single ribose-5’-phosphate moiety and PARG has been used to digest to a single ADP-ribose unit.[24–27] Investigation of mono-ADP-ribosylated proteins, however, has proven difficult because the ADP-ribose moiety fragments preferentially over the peptide backbone when using collision induced dissociation (CID). Researchers have discovered that implementing electron transfer dissociation (ETD) fragmentation techniques reduces fragmentation of the PTM and can allow for localization.[6] Furthermore, digestion to phospho-ribose by PDE or Nudix hydrolases still preserves one negatively charged phosphate group but reduces the internal fragmentation of the modification compared to ribose-5’-phosphate.

Author Manuscript Author Manuscript Author Manuscript Author Manuscript

Chemical derivitazation of ADP-ribosylation has also been used in MS approaches. Zhang et al. outlined a chemical derivatization approach utilizing hydroxylamine, which converts Glu- and Asp-ribosylated side chains to a hydroxamic acid derivative (Δm = 15.0109Da).[7] This derivative is easily tractable by mass spectrometry as it eliminates the negative charges associated with the phosphate group and does not fragment internally. However, a caveat of this approach is that it is only capable of identifying ADP-ribosylation sites on acidic residues (Glu and Asp) as these are sensitive to hydroxylamine derivatization, but is unable to derivitize other residues including Lys, Arg, and Ser.

Some of the above-described MS and sample preparation techniques have been implemented to study histone proteins. For example, the Hottiger group optimized MS parameters to identify 29 ADP-ribosylation sites on histones (Lys, Arg, Asp, and Glu residues) that were mono-ADP-ribosylated by ARTD10 *in vitro*, without derivitizing or digesting the modification.[6] More recently, Leidecker et al. analyzed histone ADP-ribosylation sites after 10 minutes of exposure to hydrogen peroxide, a potent DNA damaging agent. They were able to identify 12 novel ADP-ribosylation sites on Ser residues but did not find sites on Glu, Asp, Lys, or Arg.[2] These studies have provided critical insight into histone ADP-ribosylation; however, there still lacks a comprehensive analysis of histone ADP-ribosylation sites upon an extended DNA damage time course, and it remains unknown which of these sites are important for DNA damage repair.

Here, we characterize the histone Glu/Asp ADP-ribosylome during DNA damage using high-resolution mass spectrometry. We identified 30 histone ADP-ribosylation sites, 20 of which are novel, and quantified their abundances throughout a DNA damage time course. The results indicate that most accessible D/E sites are able to be ADP-ribosylated *in vivo* and that the abundance of these modifications increases in a time-dependent manner. To our knowledge, this is the first comprehensive analysis of histone ADP-ribosylation during DNA damage insult. The results can help elucidate how histone ADP-ribosylation sites contribute to DNA damage repair.

Materials and Methods

Cell Culture/Treatment/Histone Extraction

HeLa S3 cells were grown on plates in DMEM media supplemented with 10% newborn calf serum (Gibco), penicillin-streptomycin solution (10,000 units penicillin G and 10 mg/mL streptomycin) (Fisher) and GlutaMAX (Fisher). When indicated, cells were treated with dimethylsulfate (DMS) (Sigma) at the indicated concentration by addition to the media. Cells on 10cm plates were treated when they reached approximately 70% confluency. To harvest cells, media was removed and cells were washed with 10mL sterile PBS. Cells were removed by scraping and spun at 1000rpm for 4 minutes. PBS was removed and cells were either frozen for acid extraction, or in the case of experiments where *in nucleo* incubation was performed, nuclei were immediately extracted using hypotonic lysis. To lyse the cells, cell pellets from 10cm plates were resuspended in 5× pellet volume of ice cold buffer (1M HEPES, pH 7.9, 1M $MgCl_2$, 2.5M KCl, 1M DTT, 1× Halt protease in dH_2O) and incubated on ice for 5 minutes. Pellets were dounce homogenizied (approximately 30 strokes) and subsequently spun at 600g for 5 minutes at 4°C. Supernatant was removed and pellets

Author Manuscript Author Manuscript Author Manuscript Author Manuscript

(containing primarily nuclei) were resuspended in buffer (15mM Tris-HCL, pH 7.5, 60mM KCl, 15mM NaCl, 5mM MgCl2, 1mM CaCl2, 250mM sucrose) containing 0.2mM NAD+. Nuclei were incubated at 37°C for two hours on a rotator. Nuclei were subsequently spun at 600g for 5 minutes and the supernatant was removed. Histones were then extracted using a standard sulfuric acid extraction followed by TCA precipitation as previously described.[28–30] For all experiments where *in nucleo* incubation was not performed, nuclei were extracted from fresh or frozen pellets as previously described using detergent followed by an acid extraction and TCA precipitation.[28–30]

In Vitro ADP-ribosylation assay

Full-length human PARP-1 (residues 1 to 1014) with an N-terminal histidine tag was expressed in *E. coli* strain BL21(DE3) Rosetta2 (Novagen) and purified using three chromatographic steps (Ni^{2+}-affinity, heparin, and gel filtration) as previously reported.[31]

All *in vitro* ADP-ribosylation assays were carried out in 25uL of 50mM Tris-HCl, pH8.0, 4mM $MgCl_2$, 250uM DTT, and 20mM NaCl. Reactions contained 10pmol of recombinant wild-type PARP-1, 200 μM NAD+, 20 μg histones extracted from HeLa cells, and 10pmol of a synthesized double-stranded duplex DNA that serves to activate PARP-1. The DNA duplex was synthesized as previously described.[31] Reactions were incubated at 37°C for 30 minutes, and quenched by flash freezing.

Sample digestion

Histones extracted from untreated HeLa cells were used for optimization of histone coverage experiments. For trypsin (Promega) digests, histones were resuspended in ammonium bicarbonate, pH 8.0 to a concentration of 0.1ug/uL. Protein concentrations were measured using Bradford assays. Trypsin was added in a 1:20 enzyme:substrate ratio and incubated at 37°C for 30 minutes, 1 hour, or 1.5 hours. Reactions were quenched by lowering the pH to 4 with glacial acetic acid followed by freezing.

For chymotrypsin (Worthington) digests, histones were resuspended in ammonium bicarbonate, pH 8.0 to a concentration of 0.1ug/uL. Chymotrypsin was added in a 1:20 or 1:100 enzyme:substrate ratio and incubated at 37°C for 6 hours. Reactions were quenched by freezing.

For pepsin (Promega) digests, histones were resuspended in ammonium bicarbonate, pH 7.5 to a concentration of 0.1 ug/uL. 1N HCl was added to the solution to yield a final concentration of 0.04N. Pepsin was resuspended in double-distilled water to a final concentration of 1ug/uL and added to the sample in a 1:30 enzyme:substrate ratio. Samples were incubated at 37°C for 30 minutes, 1.5 hours, 6 hours, or overnight. Samples were quenched by addition of a small volume of 1N NaOH to increase the pH above 6.

Derivitization and desalting

In cases where samples were derivitized, hydroxylamine (Sigma) was immediately added after histone extraction to a final concentration of 1M. Samples were incubated overnight at room temperature with shaking. Samples were then desalted to remove excess

Author Manuscript Author Manuscript Author Manuscript Author Manuscript

hydroxylamine using home-made stage tip columns as previously described.[29] In this case, C8 (3M, Empore) solid phase extraction resin was used for desalting because it performs better with intact proteins compared to C18. The samples were then dried to completion in a vacuum centrifuge and resuspended in 50uL ammonium bicarbonate, pH 8.0. Trypsin (Promega) was added in a 1:20 enzyme:substrate ratio and incubated at 37°C for one hour. Digestion was quenched by addition of 5uL of glacial acetic acid to lower the pH to around 4. Samples were then desalted on home-made stage tip columns with C18 solid phase extraction resin (3M, Empore) and dried to completion in a vacuum centrifuge as previously described.[28,29]

Boronate Enrichment of ADP-ribosylated peptides

Boronate enrichment was performed when indicated on 50–100ug of digested and desalted histone samples. Samples were dried to completion in a vacuum centrifuge to remove all water residue and resuspended in 50 – 100 uL dimethyl sulfoxide (≥99.9% anhydrous, Sigma). Boronate columns (Agilent, Bond Elut PBA, 100mg) were washed with 2mL anhydrous dimethyl sulfoxide. Sample was added to the column and incubated at 35°C for 2 hours. The column was washed with 1mL anhydrous DMSO followed by 1mL acetonitrile (99.8% anhydrous, Sigma). Samples were incubated on the column with 500uL 1M hydroxylamine (Sigma) at 35°C overnight. Columns were capped to allow for longer interaction with the hydroxylamine. Desalting was subsequently performed with homemade C18 stage-tip columns.

nanoLC-MS/MS

Fused silica microcapillary tubing (75um i.d.; Polymicro Technologies) was pulled in house using a flame to generate a spray tip. Columns were packed in house with C18 resin (3 μm, Dr. Maisch GmbH, Germany). Samples were resuspended in an appropriate volume of 0.1% formic acid before being loaded onto the column using a Thermo Easy NanoLC 1000 HPLC. Peptides were separated using reversed-phase chromatography (buffer A: 0.1% formic acid in water; buffer B: 0.1% formic acid in acetonitrile) over a 60 minute gradient: 0 to 28%B in 45 minutes, 28 to 90%B in 5 minutes, 90%B for 10 minutes. For all experiments except the digest optimization, the HPLC was coupled to a hybrid linear ion trap-Orbitrap (Orbitrap Fusion, Thermo Scientific). A full MS scan ranging from 350–1500 m/z was acquired in the Orbitrap at 60,000 resolution with an AGC target of 2.0e5. MS/MS spectra of ions with an intensity greater than 5.0e3 were collected in the Orbitrap at 15,000 resolution for up to 3 seconds based on the full MS scan. Ions with a charge 2–4 were fragmented with HCD (collision energy: 27%) and ions with a charge 4–7 were fragmented with ETD using calibrated charge dependent ETD parameters. The AGC target was set to 5.0e4 for all MS/MS spectra. Dynamic exclusion was set to 25 seconds after one selection. All raw files are available on the Chorus database (ID: 1377; https://chorusproject.org/).

For the digest optimization experiment, samples were analyzed using a Thermo Q Exactive instrument with the same gradient described above. A full MS scan was collected (70,000 resolution; AGC: 1e6; maximum injection time: 50ms; scan range: 300–1,100m/z) followed by an MS/MS scan of the ten most abundant ions (resolution: 17,500; AGC: 5e4; maximum injection time: 100ms; first mass: 140 m/z; normalized collision energy: 24).

Author Manuscript Author Manuscript Author Manuscript Author Manuscript

MS Data Analysis

ETD data was searched using Mascot within Proteome Discoverer software. Files were deconvoluted using Xtract and de-isotoped spectra were searched using a database containing all human histone sequences. Deconvoluted spectra were filtered to remove precursor peaks, charge reduced precursors, neutral losses, and FT overtones. The digestion enzyme was set to semiTrypsin, and 3 missed cleavages were allowed. For digest optimization experiments, the enzyme was set to none for pepsin experiments or chymotrypsin (2 missed cleavages) for chymotrypsin digests. The precursor mass tolerance was set to 10 ppm, and the fragment mass tolerance was set to 0.04 Da. For experiments where ADP-ribosylation sites were being searched, protein N-terminal acetylation, oxidation on methionine, and hydroxamic acid on Asp/Glu were set as variable modifications. For digest optimization experiments, variable modifications were set to: acetyl (K), dimethyl (K and R), methyl (K and R), acetyl (protein N-terminus), and trimethyl (K). The target false discovery rate (FDR) was set to 0.01. All identified spectra were manually validated.

HCD data was searched using pFind Studio (version 3).[32] Thermo raw files were uploaded and searched against a database containing all human histone sequences. Trypsin was selected as the digestion enzyme, allowing up to 4 missed cleavages. The precursor tolerance was set to 10ppm and the fragment tolerance was set to 0.04Da. Methionine oxidation, protein N-terminal acetylation, and hydroxamic acid on Asp or Glu were selected as variable modifications. All identified spectra were manually validated.

Label-free quantification was performed by summing the intensities of peptides containing the modification of interest and dividing it by the sum of the intensities of peptides containing that modification site in all of its modified and unmodified forms. Intensities were obtained by calculating the area under the curve of the monoisotopic peak of the isotopic distribution of the peptide.

Results and Discussion

1. Optimization of histone digest

Histones are among the most basic proteins in the cell. Each histone contains a large number of Lys and Arg residues that are critical for interaction with the negatively charged DNA. However, this property makes histone proteins particularly challenging to study by standard MS protocols, which employ trypsin to digest proteins. Trypsin cleaves C-terminal to Lys and Arg residues, and since histones contain a large number of these residues, trypsin tends to generate very small, hydrophilic peptides that do not bind well on reversed-phase C18 columns used in most MS studies. This results in very low sequence coverage of histone proteins.

Garcia et al. developed a chemical derivitazation technique to overcome this issue.[33] In this procedure, lysine side chains are derivitized with propionic anhydride to prevent trypsin from cleaving at Lys residues. This allows for cleavage only after Arg, thereby allowing larger peptides to be generated. Additionally, the propionyl group imparts a greater hydrophobicity to the peptide, allowing better interaction with C18 resin. Unfortunately, this method is not compatible with the hydroxylamine derivatization as the resulting hydroxamic

Author Manuscript Author Manuscript Author Manuscript Author Manuscript

acid tag reacts with the propionic anhydride (data not shown). The propionylation reaction cannot be performed prior to derivization as the basicity required in the reaction will cause the labile ADP-ribosylation marks to degrade.

We therefore aimed to optimize histone sequence coverage using different digestion enzymes to enable identification of as many potential ADP-ribosylation acceptor sites as possible. We tested chymotrypsin, which cleaves C-terminal to Phe, Trp, and Tyr, pepsin, which cleaves non-specifically, and limited tryptic digests. Limiting the reaction time of trypsin will prevent the reaction from going to completion thereby generating longer peptides that will be more amenable to RP-HLPC. Previous studies indicated that H1 and H2B are the most notable acceptors of ADP-ribosylation during DNA damage so coverage of those proteins was considered more important than the other histone proteins.[19]

We performed the digests under several different conditions (Figure 1) to optimize the coverage of potential modification sites. Given that digestion patterns can vary depending on the PTM profiles of the sample (i.e. trypsin cannot cleave after acetylated Lys residues), we performed this optimization on total histones extracted from HeLa cells. Using samples collected *in vivo* also ensures that all histones variants are present.

We next performed the digestions as shown in Figure 1. For trypsin experiments, we performed limited digests of 30, 60, and 90 minutes. For pepsin, we performed digestion times of 30 minutes, 2.5 hours, 6 hours, and overnight. For chymotrypsin, we tried two different enzyme:substrate ratios including 1:100 and 1:20 as these can alter specificity. The digests were subsequently analyzed on our Thermo Q Exactive instrument.

Figure 1 demonstrates the results of the digest optimization experiments. The percent coverage is shown as an average coverage for all variants that were detected. Panel D shows the best condition for each of the three digests tested. Given that H1 and H2B are the most highly modified histones upon DNA damage, we sought to ensure high coverage of those proteins. The trypsin digest (1 hour) had the highest coverage of all histones, including H1 and H2B, compared to pepsin and chymotrypsin and also resulted in the identification of the highest number of potential modification sites (Table 1). We therefore chose to move forward with the limited trypsin digest. One caveat of this method is that data analysis is more complicated because missed cleavage sites will result in a more varied pool of peptides that must be analyzed.

2. Identification of histone ADP-ribosylation sites catalyzed by PARP-1 *in vitro*

We next sought to optimize sample preparation procedures and MS parameters for identification of ADP-ribosylation sites on histones. As noted previously, ADP-ribosylation is a particularly challenging PTM to study given that it is heterogeneous, labile, and negatively charged. We therefore opted to dervitize samples with hydroxylamine to enable identification of Asp/Glu ADP-ribosylation sites by MS.[7] Derivatization with hydroxylamine leaves a small hydroxamic acid tag (delta m = 15.0109 Da) (Figure 2A). We first wanted to determine the feasibility of this approach by analyzing histones that are ADP-ribosylated *in vitro*.

Author Manuscript Author Manuscript Author Manuscript Author Manuscript

To ADP-ribosylate histone protein *in vitro*, we developed an assay using PARP-1. We chose PARP-1 for this assay because it has been shown to be critical in DNA damage response, and its ADP-ribosylation activity is required for repairing DNA single and double strand breaks.[12,13] PARP-1 is also known to modify all five histones *in vitro*.[2,6,17–20] In the assay, histones extracted from HeLa cells were combined with PARP-1 enzyme. NAD+ was added to allow for transfer of the ADP-ribose moieties to the histones and a small double-stranded DNA segment was added to activate the PARP-1. We confirmed that the assay works by performing a western blot against poly-ADP-ribose (PAR) (Figure 2B). The results show that no ADP-ribosylation occurred when NAD+ is omitted from the reaction mixture as expected, but robust signal is detected when NAD+ is included. The resulting "smear" is characteristic of ADP-ribosylation modification because a variable number of ADP-ribose units can be added to a given site and a variable number of sites can be modified, causing the proteins to adopt a wide range of molecular weights.[19]

Given that this method can only detect Asp/Glu ADP-ribosylation sites, we sought to determine how many of these sites are modified compared to the hydroxylamine-insensitive sites (Arg, Lys, Ser) (Figure 2B). To this end, we performed an *in vitro* ADP-ribosylation assay and treated half of the sample with hydroxylamine overnight. However, in this assay, we used biotinylated NAD+ in place of unlabeled NAD+ so that streptavidin-HRP could be used as a detection reagent instead of the PAR antibody. Given that streptavidin-HRP can detect a single biotinylated ADP-ribose unit while the PAR antibody requires a small chain of ADP-ribose, this method allows for more robust detection. PARP-1 is still able to catalyze ADP-ribosylation using biotinylated NAD+. Derivatization with hydroxylamine will cause the modification (and therefore biotin tag) to be removed from Asp/Glu residues and signal will therefore decrease. However, hydroxylamine-insensitive sites will not be affected by treatment, allowing signal to be retained. Treatment with hydroxylamine demonstrated a near complete depletion of signal, indicating that a vast majority of histone ADP-ribosylation sites are occurring on Glu/Asp residues in this assay. To ensure that the hydroxylamine is not chemically modifying histone proteins, we performed a control experiment where we incubated recombinant histone proteins with hydroxylamine overnight. We did not identify any derivitized sites, indicating that the hydroxylamine does not chemically modify Asp and Glu residues on histones (data not shown). Therefore, the hydroxylamine derivatization is a suitable method to comprehensively analyze histone ADP-ribosylation sites.

We next digested the hydroxylamine dervitized samples from the PARP-1 ADP-ribosylation assay with trypsin for one hour and performed high-resolution MS/MS analysis on our Thermo Orbitrap Fusion instrument. Given that histone peptides tend to be highly charged due to the large number of Lys/Arg residues, we created an instrument method that performs electron transfer dissociation fragmentation on peptides containing charge +4 or higher. HCD fragmentation was used for peptides with charges +2 to +4. We were able to identify 7 modification sites (Table 2). However, well-characterized ADP-ribosylation sites, such as H1E2 and H1E15, were not detected in this experiment.[21] Additionally, we did not detect any modification sites on H2A or H3, despite the fact that it is known that PARP-1 is capable of modifying this histone.

Author Manuscript Author Manuscript Author Manuscript Author Manuscript

There are several possible explanations of why more sites were not identified. Since this was an *in vitro* study, we did not have the full complement of ART enzymes. There could be other sites that are not catalyzed by PARP-1 that were not detected. Secondly, PARP-1 may require some effector proteins to achieve its full function that are not present in this *in vitro* assay. Thirdly, these tests were performed on unfolded histones. Folded substrate with their native PTM profiles may be required for full modification by PARP-1. Lastly, the modifications may be of too low abundance in these *in vitro* experiments to be accurately identified by MS. However, these studies nonetheless demonstrated the utility of the hydroxylamine derivatization strategy and enabled us to develop a MS platform for analysis on more physiologically relevant samples.

3. *In nucleo* incubation with NAD+ leads to spurious ADP-ribosylation of histone proteins

To overcome the drawbacks of the *in vitro* assay, we next decided to identify modification sites *in vivo*. However, given that ADP-ribosylation is a low abundance modification (particularly when compared to canonical PTMs like acetylation), we aimed to increase the abundance of the modification *in nucleo* to facilitate identification. To this end, we supplied additional NAD+ to isolated nuclei from DMS-treated cells (Figure 3A) to enable additional ADP-ribosylation of histones. NAD+, which is impermeable to the outer cell membrane, can permeate through the nuclear membrane. These *in nucleo* experiments are common in chromatin biology field, especially with studies using radiolabeled NAD+ as it enables the radiolabeled NAD+ to easily enter the nucleus.[17,19,22]

Since histone ADP-ribosylation levels are extremely low under normal cellular conditions, we treated the cells with dimethylsulfate (DMS), a potent DNA damaging agent. DMS alkylates purine bases, which are then repaired using the base excision repair (BER) pathway.[34] We treated cells with 0.2mM DMS for 0, 10, 30, 60, and 120 minutes and immediately extracted the nuclei using hypotonic lysis. We then added 0.2mM NAD+ to the nuclei for 2 hours at 37°C to allow for more modification to occur and extracted the histones. Analysis by western blot demonstrates a high degree of PARylation across all time points, even in the untreated control (Figure 3B). This result was unexpected because it has been reported that basal levels of PARylation on histones are extremely low.[12] From there, we performed the limited trypsin digest followed by high-resolution MS/MS analysis. We were able to identify 16 sites. We quantified 5 of these sites across the time points (Figure 3C), and saw that the abundance was consistently high across time points. We expected to see an increase in abundance with treatment time as there is more accumulation of DNA damage over time. We believe that this unexpected result is due to the *in nucleo* incubation with NAD+. Flooding the cell with substrate can lead to excessive ART activity, well beyond the normal basal levels.

We next sought to assess how much ADP-ribosylation is due to the *in nucleo* incubation with NAD+ compared to normal basal levels of ADP-ribosylation. To this end, we harvested untreated HeLa cells and subjected them to the same *in nucleo* NAD+ incubation followed by histone extraction or we directly extracted histones without the *in nucleo* incubation step. We then performed a Western blot against PAR (Figure 3D) and found that the level of ADP-ribosylation in the cells that were incubated with NAD+ had a much larger degree of ADP-

Author Manuscript Author Manuscript Author Manuscript Author Manuscript

ribosylation compared to the cells that did not undergo this process. Therefore, although the *in nucleo* NAD+ incubation increased ADP-ribosylation levels to a more detectable threshold, it should not be used for quantification as it artificially increases ADP-ribosylation levels. This step may lead to modification of sites that would otherwise be unmodified at normal cellular levels of NAD+.

4. Boronate enrichment enhances identification of ADP-ribosylation sites

Given that the *in nucleo* NAD+ incubation led to spurious histone ADP-ribosylation, we sought a different method to enrich modifications for identification. We implemented boronate chromatography to accomplish this goal, as has been previously cited in the literature.[7] Boronate covalently binds cisdiols, which are present in the ADP-ribose modification (Figure 4A). Stringent washes can therefore be used to remove peptides that do not contain ADP-ribosylation. Peptides were eluted with hydroxylamine overnight and analyzed by high-resolution MS/MS.

In normal physiological conditions, histone ADP-ribosylation levels are very low, although basal levels of histone ADP-ribosylation are critical for some nuclear processes, including transcription and chromatin structure regulation.[35–37] To test the utility of boronate enrichment for identification of histone ADP-ribosylation, we decided to analyze a sample in which ADP-ribosylation levels are low because these will be the most difficult sites to detect. To this end, we collected a HeLa cell pellet under standard growing conditions and extracted histones. We then digested the histones and enriched the sample with boronate chromatography, reserving a portion of the sample to run as a control (called “input”). Samples were incubated with 1M hydroxylamine on-column overnight to allow dissociation with the boronate resin as well as derivatize the modification. Samples were eluted from the column by pushing more hydroxylamine through the column (called “elution”).

The results indicate that the boronate enrichment did allow for a larger number of modified peptides to be identified in the elution sample compared to the input (28 sites compared to 14, respectively; Figure 4B). We show the chromatograms of an example peptide from H1.2 in input and enriched samples (Sequence: KASGPPVSELITK, unmodified $[M+2H]^{2+}$ = 663.885, modified $[M+2H]^{2+}$ = 671.301) (Figure 4C). This peptide underwent a 12.4-fold enrichment after boronate chromatography, which enabled it to be detected by MS. These results indicate that boronate is an effective means to enrich ADP-ribosylated peptides under normal growing conditions to facilitate identification by MS. However, quantification of ADP-ribosylation sites must be done in non-enriched samples as the abundance of the unmodified peptide is critical for relative quantification calculations.

5. Identification and quantification of histone ADP-ribosylation levels during DMS-induced DNA damage timecourse

ART enzymes are critical for DNA damage repair. PARP-1 and PARP-2 directly bind to single and double strand breaks to ADP-ribosylate a myriad of acceptor proteins in the nucleus, including themselves, allowing DNA damage repair proteins to be recruited to the site of damage.[38] This activity has been shown to be crucial for nearly all DNA repair pathways such as homologous recombination (HR), non-homologous end-joining (NHEJ),

Author Manuscript Author Manuscript Author Manuscript Author Manuscript

and alternative-NHEJ (alt-NHEJ).[39] While the role of ART enzymes in DNA damage repair has been well studied, the role of ADP-ribosylated acceptor proteins in these processes remains unclear. Several studies have aimed to comprehensively identify ADP-ribose acceptor proteins upon various modes of DNA damage and cellular stress (e.g.[7,24,27]). For example, Daniels et al. used phosphodiesterase enzymes (PDE) followed by phopho-enrichment strategies to enrich ADP-ribosylated peptides, which were subsequently analyzed by MS for identification.[24] Histone proteins have emerged from these studies as a major acceptor of ADP-ribosylation. However, how modified histones contribute to the DNA damage response (DDR) and subsequent repair has not been established.

The first step towards elucidating the role of histone ADP-ribosylation in these processes is to understand where the modifications occur. Recently, Leidecker *et al.* analyzed histone ADP-ribosylation sites in human osteosarcoma cells in response to treatment with hydrogen peroxide.[2] They used a Nudix hydrolase to convert ADP-ribose modifications to phospho-ribose and were able to identify 12 novel ADP-ribosylation sites, unexpectedly all located on serine residues. However, previous studies have demonstrated that Asp and Glu are the main modified residues on histones, illuminating the need for a complete analysis of the Asp/Glu ADP-ribosylome on histones.

Here, we comprehensively analyze and quantify histone ADP-ribosylation sites during a DNA damage timecourse to understand which sites are important for mediating the DNA damage response. We used 0.2mM dimethyl sulfate (DMS), an alkylating agent, to induce DNA damage in HeLa cells over a timecourse of 10 minutes, 30 minutes, 1 hour and 2 hours. We validated that the DNA damage response was occurring by monitoring the level of H2AX phosphorylation at Ser 139 (γ-H2AX) over time by western blot (Figure 5A). γ-H2AX foci are formed rapidly, within seconds, of DNA damage and are therefore often used as a measure of the DNA damage response (DDR).[38] We found that the levels of γ-H2AX increased throughout the DMS timecourse, indicating that the cells are undergoing DNA damage and repair and that these time points are adequate for determining which ADP-ribosylation sites are involved in DNA damage response and repair processes.

Since hydroxylamine can only derivitize Asp and Glu residues, and not Ser, Arg, or Lys, we next sought to determine the extent of Asp/Glu ADP-ribosylation compared to Ser/Lys/Arg. To this end, we isolated nuclei of HeLa cells treated with 0.2mM DMS for 2 hours, incubated them with biotin-NAD+ for 2 hours at 37°C to enable biotinylation of ADP-ribosylation sites. We subsequently monitored the level of ADP-ribosylation with and without hydroxylamine treatment by Western blot using a streptavidin antibody (Figure 5B). We used biotinylated NAD+ because it has better sensitivity than PAR western blots; it can detect a single biotinylated ADP-ribose unit whereas PAR antibodies can only detect chains of ADP-ribose. We note that use of this technique does increase the background signal as we demonstrated *in nucleo* NAD+ incubation leads to higher than normal ADP-ribosylation levels. We therefore included an untreated control to determine the level of background labeling of biotinylated NAD+ in cells that are not undergoing DNA damage.

The results indicate that cells treated with DMS undergo significant histone ADP-ribosylation (lane 2), and nearly all of that modification is removed after overnight

Author Manuscript Author Manuscript Author Manuscript Author Manuscript

derivatization with hydroxylamine (lane 3), as indicated by lower levels of incorporated biotin-NAD+. The hydroxylamine-treated lane has less signal than the untreated lane (Lane 1), indicating that nearly all detectable ADP-ribosylation sites are on Asp/Glu residues.

After validating that we are able to identify a majority of histone ADP-ribosylation sites with our method, we next sought to identify which histone ADP-ribosylation sites are important for DNA damage response (DDR) and subsequent repair by base excision repair pathways (BER). To this end, we treated cells with the same DMS timecourse as mentioned above. We harvested cells, extracted histones, digested them with trypsin, and derivatized them with hydroxylamine overnight. We then performed high-resolution MS/MS analysis and were able to identify 29 sites, 10 of which had high enough abundance to accurately quantify over the timecourse (Figure 5C). Label-free quantification was achieved by summing the intensities of each peptide containing the modification of interest and dividing it by the total intensity of peptides containing that modification site in all of their modified forms. The results demonstrate that the abundance of each ADP-ribosylation site increases throughout the timecourse. This result is not surprising given that DMS will continue to damage DNA over time, causing an accumulation of DNA damage sites that will be repaired by BER pathways, each of which involves ART enzymes.

It is important to note that most of the identified ADP-ribosylation sites are located on the surface of the nucleosome (Figure 6). In fact, nearly every exposed Asp/Glu residue on the nucleosomal structure was identified in this study to be ADP-ribosylated. There are several more Asp/Glu residues that face the interior of the nucleosome that were not identified in this study or in other publications. This finding implies that ART enzymes are ADP-ribosylating nearly every accessible Asp/Glu residue on the surface of intact nucleosomes located near the site of DNA damage.

It has been shown that ADP-ribosylation destabilizes histone-DNA interactions and increases DNA accessibility.[37] It is likely that this destabilization is aided by charge repulsion between the ADP-ribose modifications and the negatively charged DNA of the nucleosome. Indeed, PARP-1 interaction with DNA is mediated in a similar fashion. PARP-1 activation leads to automodification of the enzyme as well as modification of histone proteins. This automodification has been linked to relaxation of chromatin, recruitment of DNA damage repair factors, and subsequent dissociation of the enzyme from chromatin.[1,40–42] Conformational changes within the enzyme and electrostatic repulsion aid in this dissociation from DNA.[43]

Given that nearly every accessible histone Glu/Asp residue was modified in our studies in response to DNA damage, it appears unlikely that specific Glu/Asp residues are critical for mediating DNA damage repair. Rather, it implies that ART enzymes are acting through a “brute force” mechanism whereby extensive ADP-ribosylation of any accessible acceptor residue on nucleosomes occurs to enable chromatin relaxation and accessibility of the underlying damaged DNA to allow for repair.

Author Manuscript Author Manuscript Author Manuscript Author Manuscript

Conclusion

Here, we demonstrate the first comprehensive analysis of the histone Asp/Glu ADP-ribosylome as well as quantitative analysis of histone ADP-ribosylation levels during DNA damage and repair. We found that nearly every accessible Asp and Glu residue on the nucleosomal surface is ADP-ribosylated upon treatment with DMS. Furthermore, there are many inaccessible Asp/Glu residues located in the core of the nucleosome that were not detected in this study or in the literature. Together these results suggest that ART enzymes are modifying intact nucleosomes without targeting specific Asp/Glu residues for modification. Future studies should aim to identify which ART enzymes are responsible for modification of nucleosomes as well as determining if any specific sites are required for DNA damage response or repair. However, these site-specific studies are very difficult to perform in mammalian cells due to the high copy number of histone genes. Recently, however, Rakhimova et al. was able to determine site specific roles of ADP-ribosylation on H2BE18 and H2BE19 during DNA double strand break repair in *Dictyostelium*, a slime mold which have a single copy of each histone gene.[44] Studies such as these will be needed to fully understand how histone ADP-ribosylation sites contribute to DNA damage response and repair.

Acknowledgments

Funding from NIH grants GM110174 (B.A.G), CA196539 (B.A.G), GM087282 (J.M.P), and 5 T32 GM 71339-12 (B.A.G.), and CIHR grant 142354 (J.M.P.) are gratefully acknowledged.

References

1. Hassa PO, Haenni SS, Elser M, Hottiger MO. Nuclear ADP-Ribosylation Reactions in Mammalian Cells: Where Are We Today and Where Are We Going? Microbiol. Mol. Biol. Rev. 2006; 70(3): 789–829. [PubMed: 16959969]
2. Leidecker O, Bonfiglio JJ, Colby T, Zhang Q, Atanassov I, Zaja R, Palazzo L, Stockum A, Ahel I, Matic I. Serine is a new target residue for endogenous ADP-ribosylation on histones. Nat. Chem. Biol. 2016; 12(12):998–1000. [PubMed: 27723750]
3. Altmeyer M, Messner S, Hassa PO, Fey M, Hottiger MO. Molecular mechanism of poly(ADP-ribosyl)ation by PARP1 and identification of lysine residues as ADP-ribose acceptor sites. Nucleic Acids Res. 2009; 37(11):3723–3738. [PubMed: 19372272]
4. McDonald LJ, Moss J. Enzymatic and nonenzymatic ADP-ribosylation of cysteine. Mol. Cell. Biochem. 1994; 138(1–2):221–226. [PubMed: 7898467]
5. Laing S, Unger M, Koch-Nolte F, Haag F. ADP-ribosylation of arginine. Amino Acids. 2011; 41(2): 257–269. [PubMed: 20652610]
6. Rosenthal F, Nanni P, Barkow-Oesterreicher S, Hottiger MO. Optimization of LTQ-Orbitrap Mass Spectrometer Parameters for the Identification of ADP-Ribosylation Sites. J. Proteome Res. 2015; 14(9):4072–4079. [PubMed: 26211397]
7. Zhang Y, Wang J, Ding M, Yu Y. Site-specific characterization of the Asp- and Glu-ADP-ribosylated proteome. Nat. Methods. 2013; 10(10):981–984. [PubMed: 23955771]
8. Gibson BA, Kraus WL. New insights into the molecular and cellular functions of poly(ADP-ribose) and PARPs. Nat. Rev. Mol. Cell Biol. 2012; 13(7):411–424. [PubMed: 22713970]
9. Verheugd P, Bütepage M, Eckei L, Lüscher B. Players in ADP-ribosylation: Readers and Erasers. Curr. Protein Pept. Sci. 2016; 17(7):654–667. [PubMed: 27090904]
10. Eustermann S, Wu W-F, Langelier M-F, Yang J-C, Easton LE, Riccio AA, Pascal JM, Neuhaus D. Structural Basis of Detection and Signaling of DNA Single-Strand Breaks by Human PARP-1. Mol. Cell. 2015; 60(5):742–754. [PubMed: 26626479]

Author Manuscript Author Manuscript Author Manuscript Author Manuscript

11. Langelier M-F, Planck JL, Roy S, Pascal JM. Structural basis for DNA damage-dependent poly(ADP-ribosyl)ation by human PARP-1. Science. 2012; 336(6082):728–732. [PubMed: 22582261]
12. D'Amours D, Desnoyers S, D'Silva I, Poirier GG. Poly(ADP-ribosyl)ation reactions in the regulation of nuclear functions. Biochem. J. 1999; 342(Pt 2):249–268. [PubMed: 10455009]
13. Wei H, Yu X. Functions of PARylation in DNA Damage Repair Pathways. Genomics Proteomics Bioinformatics. 2016; 14(3):131–139. [PubMed: 27240471]
14. Luger K, Mäder AW, Richmond RK, Sargent DF, Richmond TJ. Crystal structure of the nucleosome core particle at 2.8 Å resolution. Nature. 1997; 389(6648):251–260. [PubMed: 9305837]
15. Hergeth SP, Schneider R. The H1 linker histones: multifunctional proteins beyond the nucleosomal core particle. EMBO Rep. 2015; 16(11):1439–1453. [PubMed: 26474902]
16. Zhao Y, Garcia BA. Comprehensive Catalog of Currently Documented Histone Modifications. Cold Spring Harb. Perspect. Biol. 2015; 7(9):a025064. [PubMed: 26330523]
17. Riquelme PT, Burzio LO, Koide SS. ADP ribosylation of rat liver lysine-rich histone in vitro. J. Biol. Chem. 1979; 254(8):3018–3028. [PubMed: 218960]
18. Huletsky A, Niedergang C, Fréchette A, Aubin R, Gaudreau A, Poirier GG. Sequential ADP-ribosylation pattern of nucleosomal histones. Eur. J. Biochem. 1985; 146(2):277–285. [PubMed: 2981686]
19. Boulikas T. At least 60 ADP-ribosylated variant histones are present in nuclei from dimethylsulfate-treated and untreated cells. EMBO J. 1988; 7(1):57–67. [PubMed: 3359995]
20. Messner S, Altmeyer M, Zhao H, Pozivil A, Roschitzki B, Gehrig P, Rutishauser D, Huang D, Caflisch A, Hottiger MO. PARP1 ADP-ribosylates lysine residues of the core histone tails. Nucleic Acids Res. 2010; 38(19):6350–6362. [PubMed: 20525793]
21. Ogata N, Ueda K, Kagamiyama H, Hayaishi O. ADP-ribosylation of histone H1. Identification of glutamic acid residues 2, 14, and the COOH-terminal lysine residue as modification sites. J. Biol. Chem. 1980; 255(16):7616–7620. [PubMed: 6772638]
22. Adamietz P, Rudolph A. ADP-ribosylation of nuclear proteins in vivo. Identification of histone H2B as a major acceptor for mono- and poly(ADP-ribose) in dimethyl sulfate-treated hepatoma AH 7974 cells. J. Biol. Chem. 1984; 259(11):6841–6846. [PubMed: 6725273]
23. Bredehorst R, Wielckens K, Gartemann A, Lengyel H, Klapproth K, Hilz H. Two Different Types of Bonds Linking Single ADP-Ribose Residues Covalently to Proteins. Eur. J. Biochem. 1978; 92(1):129–135. [PubMed: 729585]
24. Daniels CM, Ong S-E, Leung AKL. Phosphoproteomic approach to characterize protein mono- and poly(ADP-ribosyl)ation sites from cells. J. Proteome Res. 2014; 13(8):3510–3522. [PubMed: 24920161]
25. Oka J, Ueda K, Hayaishi O. Snake venom phosphodiesterase: Simple purification with Blue Sepharose and its application to poly(ADP-ribose) study. Biochem. Biophys. Res. Commun. 1978; 80(4):841–848. [PubMed: 205220]
26. Daniels CM, Thirawatananond P, Ong S-E, Gabelli SB, Leung AKL. Nudix hydrolases degrade protein-conjugated ADP-ribose. Sci. Rep. 2015; 5:srep18271.
27. Martello R, Leutert M, Jungmichel S, Bilan V, Larsen SC, Young C, Hottiger MO, Nielsen ML. Proteome-wide identification of the endogenous ADP-ribosylome of mammalian cells and tissue. Nat. Commun. 2016; 7:ncomms12917.
28. Sidoli S, Bhanu NV, Karch KR, Wang X, Garcia BA. Complete Workflow for Analysis of Histone Post-translational Modifications Using Bottom-up Mass Spectrometry: From Histone Extraction to Data Analysis. J. Vis. Exp. JoVE. 2016; 111
29. Lin, S., Garcia, BA. Chapter One - Examining Histone Posttranslational Modification Patterns by High-Resolution Mass Spectrometry. In: Carl, Wu, David Allis, C., editors. Methods in Enzymology. Vol. 512. Nucleosomes, Histones & Chromatin Part A; Academic Press; 2012. p. 3-28.
30. Karch, KR., Sidoli, S., Garcia, BA. Chapter One - Identification and Quantification of Histone PTMs Using High-Resolution Mass Spectrometry. In: Marmorstein, R., editor. Methods in Enzymology. Vol. 574. Enzymes of Epigenetics, Part B; Academic Press; 2016. p. 3-29.

Author Manuscript Author Manuscript Author Manuscript Author Manuscript

31. Langelier M-F, Steffen JD, Riccio AA, McCauley M, Pascal JM. Purification of DNA Damage-Dependent PARPs from E. coli for Structural and Biochemical Analysis. Methods Mol. Biol. Clifton NJ. 2017; 1608:431–444.
32. Wang L, Li D-Q, Fu Y, Wang H-P, Zhang J-F, Yuan Z-F, Sun R-X, Zeng R, He S-M, Gao W. pFind 2.0: a software package for peptide and protein identification via tandem mass spectrometry. Rapid Commun. Mass Spectrom. 2007; 21(18):2985–2991. [PubMed: 17702057]
33. Garcia BA, Mollah S, Ueberheide BM, Busby SA, Muratore TL, Shabanowitz J, Hunt DF. Chemical derivatization of histones for facilitated analysis by mass spectrometry. Nat. Protoc. 2007; 2(4):933–938. [PubMed: 17446892]
34. Cabelof DC, Raffoul JJ, Yanamadala S, Ganir C, Guo Z, Heydari AR. Attenuation of DNA polymerase β-dependent base excision repair and increased DMS-induced mutagenicity in aged mice. Mutat. Res. 2002; 500(1–2):135. [PubMed: 11890943]
35. Murcia, G de, Huletsky, A., Lamarre, D., Gaudreau, A., Pouyet, J., Daune, M., Poirier, GG. Modulation of chromatin superstructure induced by poly(ADP-ribose) synthesis and degradation. J. Biol. Chem. 1986; 261(15):7011–7017. [PubMed: 3084493]
36. Niedergang CP, de MURCIA G, Ittel M-E, Pouyet J, Mandel P. Time course of polynucleosome relaxation and ADP-ribosylation. Eur. J. Biochem. 1985; 146(1):185–191. [PubMed: 3917919]
37. Martinez-Zamudio R, Ha HC. Histone ADP-Ribosylation Facilitates Gene Transcription by Directly Remodeling Nucleosomes. Mol. Cell. Biol. 2012; 32(13):2490–2502. [PubMed: 22547677]
38. Sharma A, Singh K, Almasan A. Histone H2AX phosphorylation: a marker for DNA damage. Methods Mol. Biol. Clifton NJ. 2012; 920:613–626.
39. Pears CJ, Couto CA-M, Wang H-Y, Borer C, Kiely R, Lakin ND. The role of ADP-ribosylation in regulating DNA double-strand break repair. Cell Cycle Georget. Tex. 2012; 11(1):48–56.
40. Mortusewicz O, Amé J-C, Schreiber V, Leonhardt H. Feedback-regulated poly(ADP-ribosyl)ation by PARP-1 is required for rapid response to DNA damage in living cells. Nucleic Acids Res. 2007; 35(22):7665–7675. [PubMed: 17982172]
41. Ferro AM, Olivera BM. Poly(ADP-ribosylation) in vitro. Reaction parameters and enzyme mechanism. J. Biol. Chem. 1982; 257(13):7808–7813. [PubMed: 6282854]
42. Strickfaden H, McDonald D, Kruhlak MJ, Haince J-F, Th'ng JPH, Rouleau M, Ishibashi T, Corry GN, Ausio J, Underhill DA, et al. Poly(ADP-ribosyl)ation-dependent Transient Chromatin Decondensation and Histone Displacement following Laser Microirradiation. J. Biol. Chem. 2016; 291(4):1789–1802. [PubMed: 26559976]
43. Steffen JD, McCauley MM, Pascal JM. Fluorescent sensors of PARP-1 structural dynamics and allosteric regulation in response to DNA damage. Nucleic Acids Res. 2016; 44(20):9771–9783. [PubMed: 27530425]
44. Rakhimova A, Ura S, Hsu D-W, Wang H-Y, Pears CJ, Lakin ND. Site-specific ADP-ribosylation of histone H2B in response to DNA double strand breaks. Sci. Rep. 2017; 7:43750. [PubMed: 28252050]
45. Iwasaki W, Miya Y, Horikoshi N, Osakabe A, Taguchi H, Tachiwana H, Shibata T, Kagawa W, Kurumizaka H. Contribution of histone N-terminal tails to the structure and stability of nucleosomes. FEBS Open Bio. 2013; 3:363–369.

Author Manuscript Author Manuscript Author Manuscript Author Manuscript

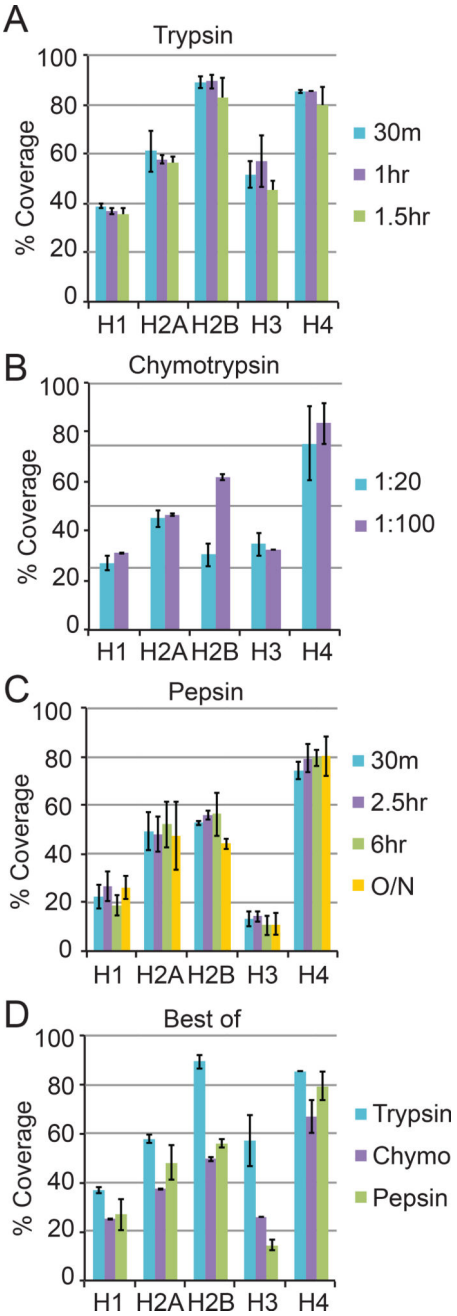

Figure 1.

Optimization of histone coverage. Histones extracted from HeLa cells were digested by proteases under several different experimental conditions to optimize coverage. The coverage obtained for each histone type are shown for trypsin (A), pepsin (B), and chymotrypsin (C). Values represent an average coverage value for all detected histone variants. The color of each bar indicates the experimental condition as shown in the key. Panel D shows the experimental condition with the highest coverage for each protease tested. Error bars represent the standard deviation of three experimental replicates.

Author Manuscript Author Manuscript Author Manuscript Author Manuscript

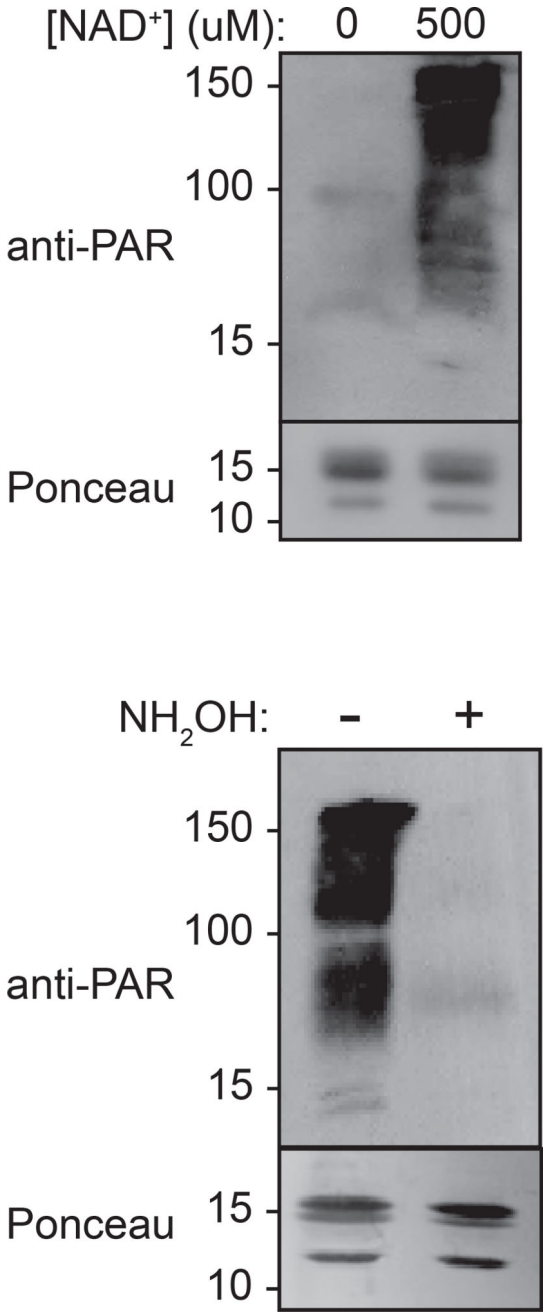

Figure 2.

PARP-1 ADP-ribosylates Asp and Glu residues of histone proteins *in vitro*. (A) *in vitro* PARP-1 assay effectively ADP-ribosylates histone proteins. Total histones extracted from HeLa cells (20ug) were incubated with PARP-1 and a short double-stranded DNA molecule with or without NAD+ for 30 minutes at 30°C. The reaction was quenched by freezing and a Western blot against poly-ADP-ribose was performed. Prior to transfer, membranes were stained with Ponceau to verify equal loading between lanes. (B) Histone ADP-ribosylation occurs predominantly on Asp/Glu residues. The same *in vitro* PARP-1 assay was performed on 40 ug of histones extracted from HeLa cells. Half of the sample was incubated with 1M

Author Manuscript Author Manuscript Author Manuscript Author Manuscript

hydroxylamine overnight at room temperature. A Western blot against poly-ADP-ribose was performed to monitor incorporation of ADP-ribosylation.

Author Manuscript Author Manuscript Author Manuscript Author Manuscript

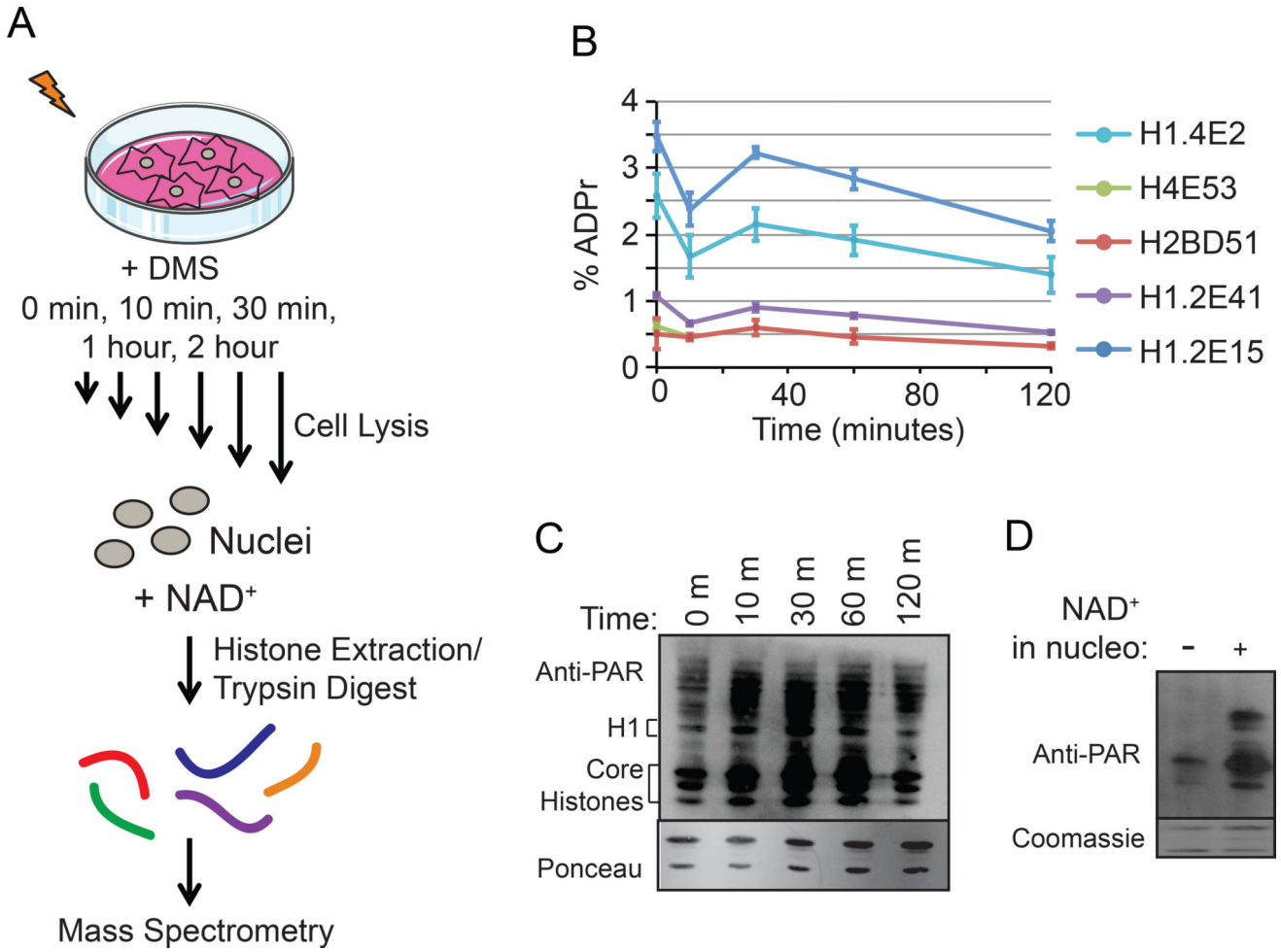

Figure 3.

Incubation of HeLa nuclei with NAD+ leads to spurious ADP-ribosylation. (A) General workflow used to identify histone ADP-ribosylation sites. HeLa cells were treated with 0.2mM DMS for indicated time points, hypotonically lysed, and incubated with 0.2mM NAD+ for 2 hours at 37°C. (B) Histone ADP-ribosylation levels remain constant over the DMS timecourse. Five example ADP-ribosylation sites were quantified and normalized to the abundance of the non-modified peptide. Error bars represent the standard deviation of three experimental replicates. (C) Histones are highly ADP-ribosylated upon incubation with NAD+ *in nucleo.* A Western blot against poly-ADP-ribose was performed on histones extracted from HeLa cells during the DMS timecourse. (D) Histones undergo a larger degree of ADP-ribosylation when incubated with NAD+ *in nucleo* compared to histones extracted from intact cells. A Western blot against poly-ADP-ribose was performed on histones extracted from HeLa cells with or without *in nucleo* incubation with NAD+.

Author Manuscript Author Manuscript Author Manuscript Author Manuscript

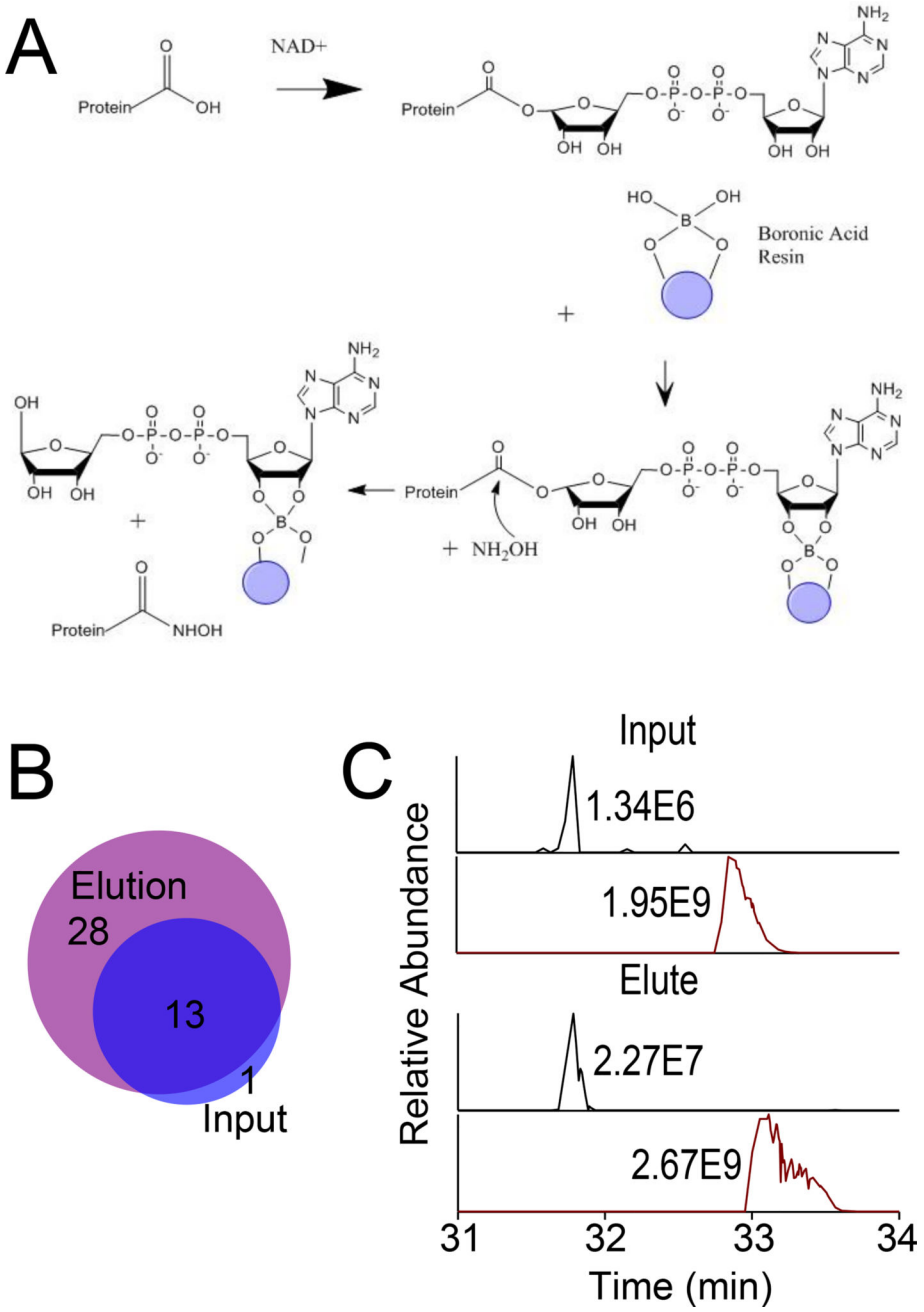

Figure 4.

Boronate enrichment enables identification of low-level ADP-ribosylation sites on histones. (A) Mechanism of covalent interaction between boronate and cis-diols of an ADP-ribose modification. Hydroxylamine removes ADP-ribose modifications on acidic residues by nucleophilic attack at the carbonyl group of the resulting ester bond. (B) Comparison of sites identified in input and enriched samples. (C) Boronate enrichment increases the abundance of modified peptides relative to unmodified peptides. Extracted ion chromatograms (XICs) are displayed for the peptide (Sequence: KASGPPVSELITK, H1.2) in its modified (hydroxamic acid, top trace, black, $[M+2H]^{2+}$ = 671.301) and unmodified (bottom trace,

Author Manuscript Author Manuscript Author Manuscript Author Manuscript

maroon, $[M+2H]^{2+}$ = 663.885) forms. The top figure represents XICs from input sample and the bottom figure represents XICs from the elution sample. The peptide shown here underwent a 12.4-fold enrichment.

Author Manuscript Author Manuscript Author Manuscript Author Manuscript

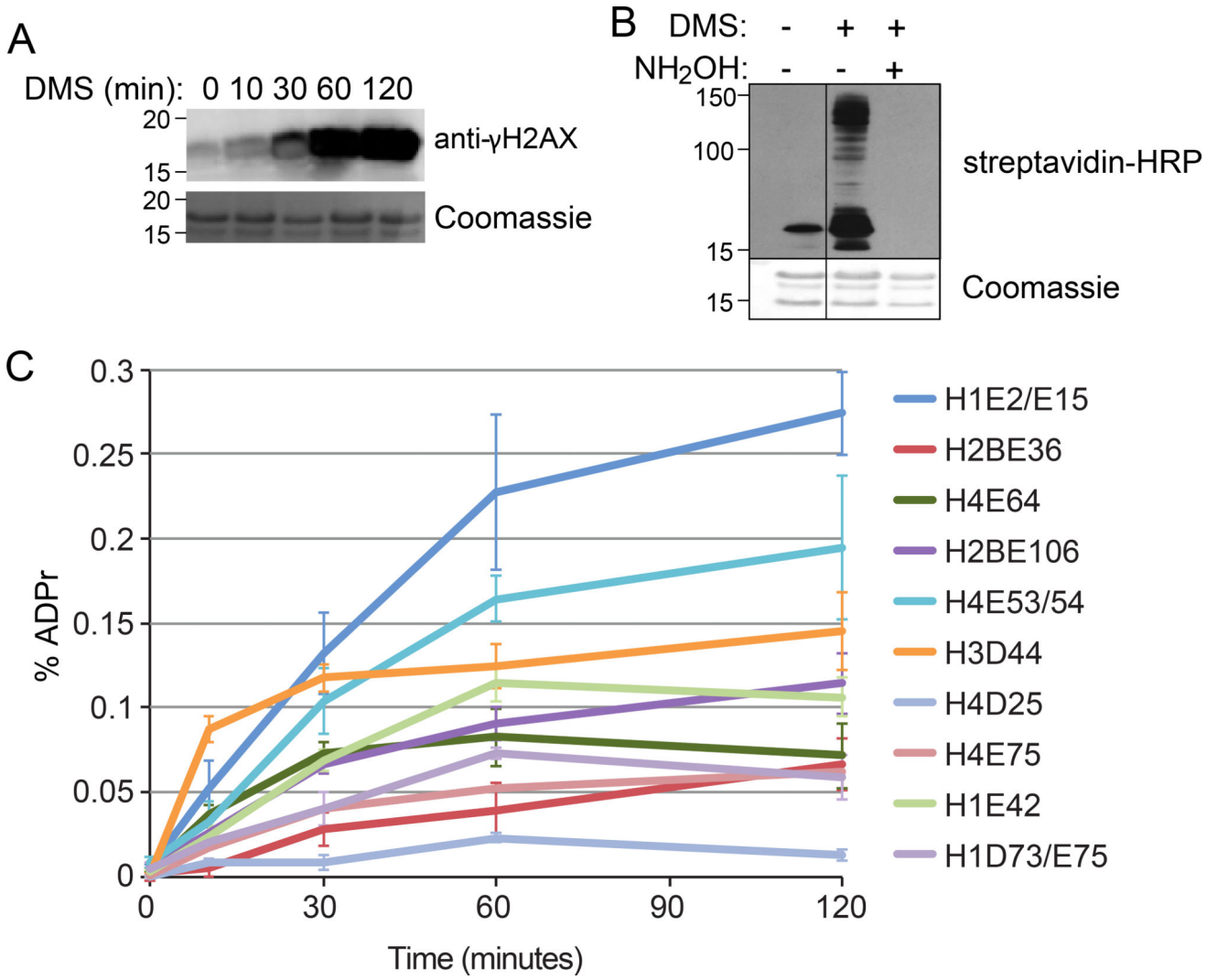

Figure 5.

Histone ADP-ribosylation levels increase with the amount of DNA damage. (A) DMS treatment leads to an extensive DNA damage response. Histones were extracted from cells undergoing DNA damage by DMS treatment. A Western blot against H2AX phosphorylated at Ser139 (γH2AX) was performed. (B) Most histone ADP-ribosylation in response to DMS damage occurs on Asp/Glu residues. Cells were treated with 0.2mM DMS for 2 hours, nuclei were extracted and incubated with biotin-NAD+. A portion of the sample was incubated with 1M hydroxylamine overnight at room temperature with shaking. A Western blot using streptavidin-HRP was used to visualize the extent of ADP-ribosylation. Lanes 2 and 3 of the blot were removed because they were not relevant. The blot and Coomassie stains show lanes 1, 4, and 5 of the original Western blot. (C) Histone ADP-ribosylation levels increase throughout DNA damage timecourse. Ten ADP-ribosylation sites were quantified and plotted on the graph. Error bars represent the standard error of 5 biological replicates. Label-free quantification was performed by normalizing the abundance of the peptide containing an ADP-ribosylation site to the abundance of the peptide in all of its modified and unmodified forms.

Author Manuscript Author Manuscript Author Manuscript Author Manuscript

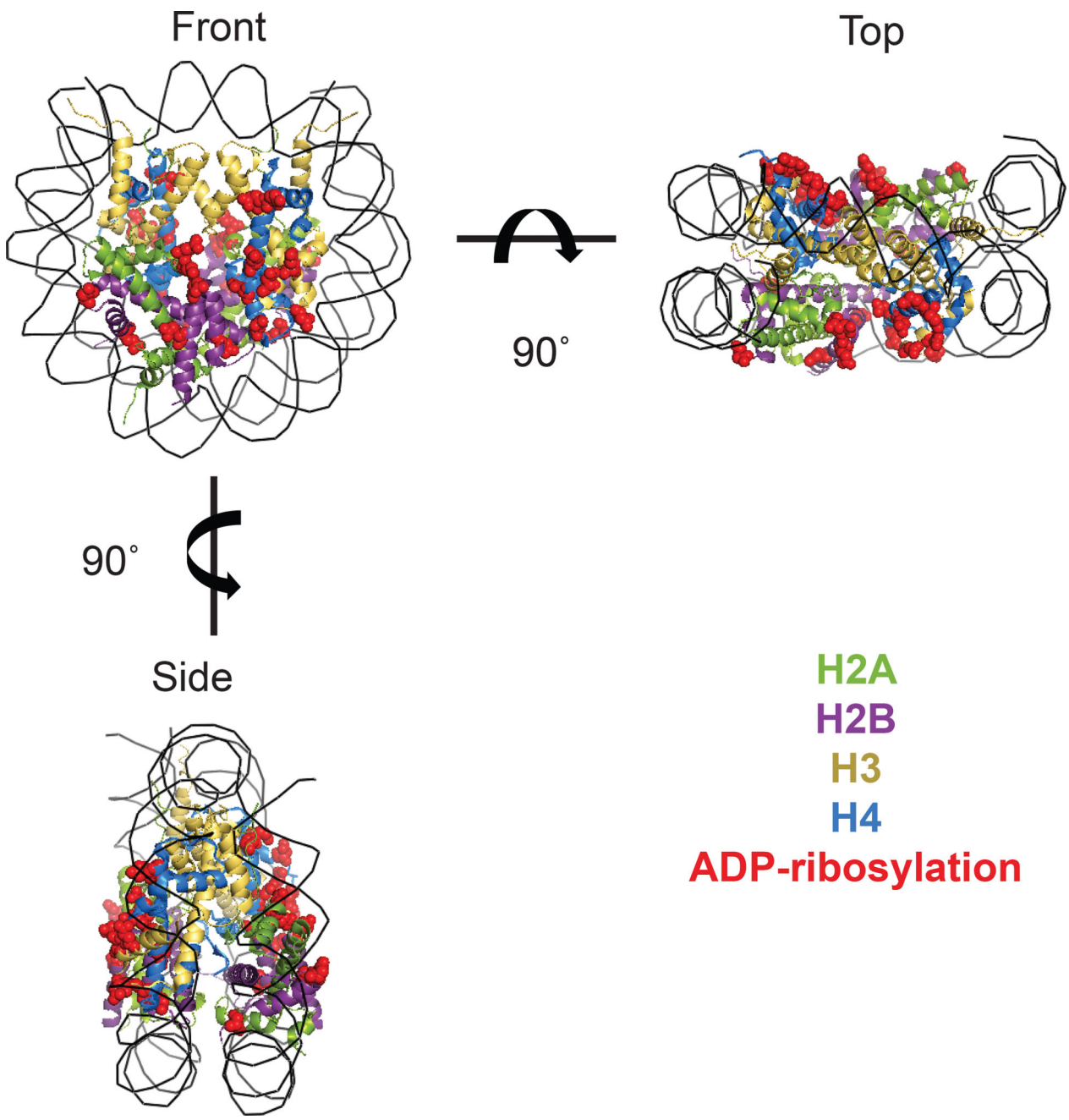

Figure 6.

ADP-ribosylation occurs primarily on the surface of the nucleosome. The crystal structure of the human nucleosome containing H3.1, H4, H2A type 1-B/E, and H2B type 1-J (PDB: 3W98) is shown.[45] The histones are colored according to the legend, with Asp/Glu residues that were found to be ADP-ribosylated shown in red spheres. Note that PDB structure does not contain full length histones and so not all identified sites are displayed in the figure (structure contains H3.1: AA 38–136, H4: 19–104, H2A type 1-B/E: 13–118, H2B type 1-J: 30–124).

Author Manuscript Author Manuscript Author Manuscript Author Manuscript

Table 1

Histone coverage optimization.

Histone		Pepsin	Chymotrypsin	Trypsin
H1	Coverage	26.53%	24.90%	36.57%
	# missing	2	4	0
	# included	5	3	7
H2A	Coverage	48.03%	37.19%	57.66%
	# missing	4	4	1
	# included	5	5	8
H2B	Coverage	56.01%	49.41%	89.33%
	# missing	4	4	1
	# included	6	6	9
H3	Coverage	14.21%	25.74%	56.77%
	# missing	8	7	6
	# included	3	4	5
H4	Coverage	79.29%	66.99%	85.44%
	# missing	0	0	0
	# included	7	7	7
Total	# missing	18	19	8
	# included	26	25	36

Rows labeled “# missing” and “# included” indicate the number of Asp/Glu sites that were not covered or included in the identified peptides, respectively, from the isoform with the highest coverage. The coverage values are given as an average of the identified histone variants.

Author Manuscript Author Manuscript Author Manuscript Author Manuscript

Table 2

Identified ADP-ribosylation sites.

#	Histone	Site	Sequence	Peptide m/z	z	Parent Mass	Score	Accession	in vivo?	in vitro?	Source
1	H1.1	E55	ERGGVSLAALK	558.331	2	1115.655	4.51E-04	Q02539	Y		
2	H1.2	E2	S(Ac)ETAPAAPAAAPPAEK	768.389	2	1535.771	4.60E-05	P16403	Y		1
			S(Ac)ETAPAAPAAAPPAEKAPVK	966.015	2	1931.023	1.02E-03	P16403			
3	H1.2	E15	S(Ac)ETAPAAPAAAPPAEK	768.389	2	1535.770	8.68E-05	P16403	Y		1
4	H1.2	E41	ASGPPVSELITK	607.343	2	1213.679	6.22E-04	P16403	Y	Y	
			KASGPPVSELITK	671.390	2	1341.773	6.76E-05	P16403			
			KASGPPVSELITK	447.930	3	1341.773	4.24E-04	P16403			
5	H1.2	E52	ERSGVSLAALK	573.337	2	1145.667	4.29E-04	P16403	Y		
6	H1.2	D71	ALAAAGYDVEK	561.794	2	1122.581	1.79E-04	P16403	Y		
7	H1.2	E73	ALAAAGYDVEK	561.794	2	1122.581	2.90E-04	P16403	Y		
			KALAAAGYDVEK	625.840	2	1250.673	3.81E-05	P16403			
8	H1.4	E2	SETAPAAPAAPAPAEK	747.387	2	1493.766	2.98E-03	P10412	Y		
9	H1.5	D74	ALAAGGYDVEKNNSR	790.392	2	1579.776	9.80E-03	P16401	Y		
			KALAAGGYDVEKNNSR	569.960	3	1707.865	1.73E-01	P16401			
10	H1.5	E76	ALAAGGYDVEK	554.784	2	1108.560	2.00E-02	P16401	Y		
			ALAAGGYDVEKNNSR	790.390	2	1579.773	7.96E-02	P16401			
			KALAAGGYDVEKNNSR	569.961	3	1707.866	3.64E-02	P16401			

Author Manuscript Author Manuscript Author Manuscript Author Manuscript

#	Histone	Site	Sequence	Peptide m/z	z	Parent Mass	Score	Accession	in vivo?	in vitro?	Source
11	H1.5	D74&E76	ALAAGGYDVEKNNSR	797.894	2	1594.780	5.83E-02	P16401	Y		
			ALAAGGYDVEK	562.285	2	1123.562	3.62E-01	P16401			
12	H2A2B	D90	HLQLAVRNDEELNK	565.300	3	1693.885	7.12E-04	Q8IUE6	Y		
13	H2A2B	D90&E91	HLQLAVRNDEELNK	854.953	2	1708.899	1.52E-02	Q8IUE6	Y		2 (E91)
14	H2AZ	D93	GDEELDSLIK	567.287	2	1133.567	3.30E-02	P0C0S5	Y		
15	H2B1C	E35	KESYSVYVYK	640.832	2	1280.656	1.87E-02	P62807	Y		2
16	H2B1C	D51	QVHPDTGISSK	395.208	3	1183.607	8.13E-03	P62807	Y		
17	H2B1C	E93	EIQTAVR	416.235	2	831.462	4.11E-01	P62807	Y		
18	H2B1C	E105	LLLPGELAK	484.811	2	968.614	4.39E-03	P62807	Y	Y	2
19	H2B1C	E113	HAVSEGTKAVTKYTSSK	603.655	3	1808.949	2.16E-02	P62807	Y		
20	H2B3B	E93	STITSREVQTAVR	731.898	2	1462.788	8.77E-03	Q8N257	Y		
21	H3.1	E59	STELLIR	423.756	2	846.505	3.26E-03	P68431		Y	
22	H3.1	E73	EIAQDFKTDLR	450.906	3	1350.701	2.07E-02	P68431	Y	Y	
23	H3.1	D77	EIAQDFK	433.224	2	865.441	4.49E-02	P68431	Y		2
			EIAQDFKTDLR	675.849	2	1350.691	3.82E-01	P68431			
			EIAQDFKTDLR	450.902	3	1350.690	1.94E-01	P68431			
24	H3.1	D81	EIAQDFKTDLR	675.858	2	1350.709	2.99E-01	P68431	Y		
25	H4	D24	DNIQGITKPAIR	447.591	3	1340.758	1.20E-03	P62805	Y		

Author Manuscript Author Manuscript Author Manuscript Author Manuscript

#	Histone	Site	Sequence	Peptide m/z	z	Parent Mass	Score	Accession	in vivo?	in vitro?	Source
26	H4	E52	ISGLIY**E**ETR	598.321	2	1195.634	4.06E-03	P62805	Y	Y	2
27	H4	E53	ISGLIYE**E**TR	598.321	2	1195.634	1.64E-03	P62805	Y	Y	2
28	H4	E63	VFL**E**NVIR	502.798	2	1004.589	1.32E-02	P62805	Y		2
29	H4	D68	**D**AVTYTEHAK	575.281	2	1149.554	2.32E-03	P62805	Y		
30	H4	E74	DAVTYT**E**HAK	575.281	2	1149.555	1.67E-03	P62805	Y	Y	2,3

The modified residue is shown in bold red. (Ac) indicates protein N-terminal acetylation. In columns “in vivo” and “in vitro”, the Y (standing for “Yes”) designation indicates that the peptide was found in the respective experiments. The column labeled “z” represents the charge of the peptide. The column labeled “source” indicates in which previous studies, if any, identified that modification (1 = Ogata et al., 1980. 2= Rosenthal et al., 2015. 3= Zhang et al., 2013).